AT THE ENTERPRISES AND INSTITUTES

UDC 666.189.211:666.94:620.193

PREDICTION OF CHANGES IN THE STRENGTH OF FIBERGLASS-CEMENT COMPOSITES WITH TIME

F. N. Rabinovich[1]

A method for predicting variations in the carrying capacity of composites based on cement matrices using different types of fiberglass as reinforcing components is developed. The method can be used in designing fiberglass-cement building structures intended for long-time service.

In the development of methods for analysis of fiberglass-cement structures, one should take into account the decrease in the strength of fiberglass with time due to its corrosion in cement matrices [1, 2].

The tensile strength of a composite for the case of rigid fixation of fibers to the matrix is expressed in the form of the known relationship

$$\sigma_c = \sigma_m \mu_m + \sigma_f \mu_f, \tag{1}$$

where σ_c, σ_m, and σ_f are the tensile strength of the composite, the matrix, and the fibers, respectively; μ_m and μ_f are the volume parts of the matrix and the reinforcing fibers in the composite.

Due to corrosion under the effect of an alkaline medium of hydrated cement, the effective diameter of fibers and the surface area of their cross-lateral (working) section decrease. These modifications are represented as a function related to decreasing strength of fiber, although in fact as the section of the fiber decreases, the force they can absorb decreases (due to decreasing m_f in the composite), provided that strength (rupture stress) is arbitrarily constant for each particular fiber (for any site of its cross-section), regardless of the corrosion process.

To take into account these circumstances, let us introduce the coefficient of service conditions m_{dur} into formula (1):

$$\sigma_c = \sigma_m \mu_m + \sigma_f m_{dur} \mu_f.$$

The purpose of the present study is to develop an analytic method for estimating the coefficient m_{dur}. Not only determination of long-time strength of reinforcing fibers but also determination of their strength at any given moment are of practical interest. Therefore, the coefficient m_{dur} should be represented as a function of time:

$$m_{dur} = m_{dur}(\tau).$$

To solve the considered problem, we used the results of earlier experimental studies [3] and experimental studies of other researchers [4 – 14].

In the first stage of research in [3] the initial (effective) fiber diameter d_{f_0} and rupture stress P_0 were determined:

$$P_0 = \frac{4N_{exp}}{\pi d_{f_0}^2}, \tag{2}$$

where N_{exp} is the fiber rupture force.

In the second phase, after holding fiber in a saturated $Ca(OH)_2$ solution simulating the effect of the alkaline medium of hydrated cement, the real fiber diameter $d_{f\tau}$ and rupture stress P_τ were determined:

$$P_\tau = \frac{4N_{exp}}{\pi d_{f\tau}^2}. \tag{3}$$

Let us assume that the decreased strength of fibers is a consequence of a decrease in their effective cross-section caused by corrosion of glass. In this case using formulas (2) and (3) we obtain

$$d_{f\tau} = d_{f_0} \sqrt{\frac{P_\tau}{P_0}}.$$

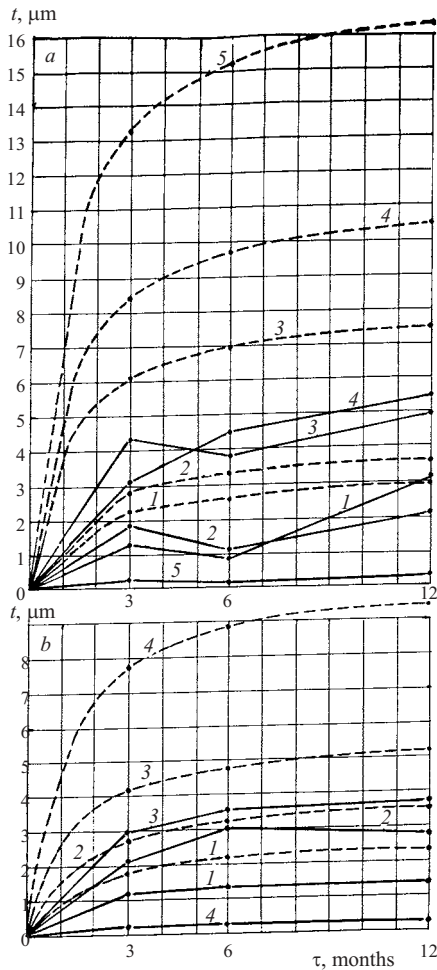[1] TsNIIpromzdanii Join-Stock Company, Russia.

Fig. 1. Experimental data (solid curves) and estimated values (dashed curves) of thickness t of the conventional fiber layer corroded in saturated solution of $Ca(OH)_2$: *a*) aluminoborosilicate fibers of diameters 6.5 (*1*), 10.3 (*2*), 46.0 (*3*), 90.1 (*4*), and 219.0 μm (*5*); *b*) basalt fibers of diameters 6.7 (*1*), 15.1 (*2*), 33.4 (*3*), and 117.0 μm (*4*).

The thickness t of a conventional glass layer that is destroyed as a consequence of corrosion is equal to

$$t = \frac{d_{f_0} - d_{f\tau}}{2}. \qquad (4)$$

The values of the conventional layer t is convenient for analytical description taking into account its variation (increase) with time [15]. The values t calculated according to formula (4) on the basis of fiber testing data are shown in Fig. 1. On the whole, the obtained curves $t - \tau$ are ascending; moreover, corrosion grows most intensely in the first three months and then slows down.

It was earlier established [16] that as the fiber diameter grows, the mass of CaO absorbed by a fiber surface unit increases. This is also corroborated by the results of experimental studies [3]. The greater the mass of CaO assimilated
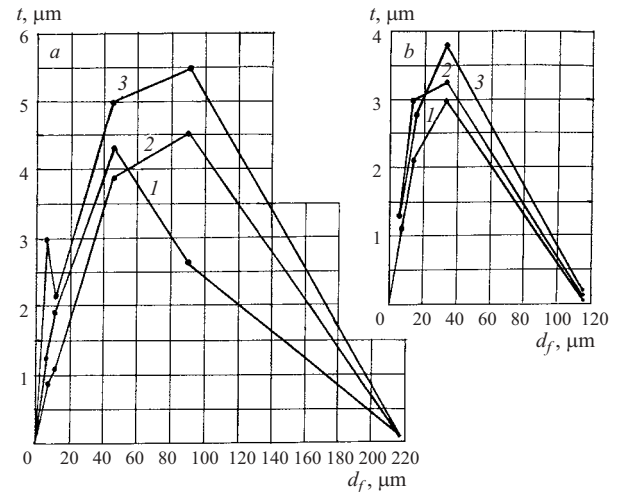

Fig. 2. Variation of dependence $t - d_f$ with time: *a*) fibers E; *b*) basalt fibers; *1*, *2*, and *3*) 3, 6, and 12 months, respectively.

by a fiber surface area unit, the larger the thickness of the conventional glass layer and the more intense the corrosion process (Fig. 1). It can be seen that up to certain limits (at $d_f \le 80 - 100$ μm) the absorbed CaO mass grows almost linearly with increasing fiber diameter; at $d_f > 80 - 100$ μm this process slows down and attenuates. The relationships $t - d_f$ have a similar nature (Fig. 2).

It is interesting to consider the fiber parameters after their reaction for 12 moths with a saturated calcium hydroxide solution (Fig. 3). These dependences were constructed using the data in [3]. In doing so, the volumes and mass parts of aluminoborosilicate and basalt fibers, both corroded and intact, were estimated.

The intact fiber volumes were calculated from the formula

$$V_{f\tau\,c} = \frac{d_{f\tau}^2 V_{f_0}}{d_{f_0}^2},$$

where $d_{f\tau} = d_{f_0} - 2t$; $V_{f_0} = 1/\rho_f = 0.385$ cm³ for aluminoborosilicate fibers and $V_{f_0} = 0.357$ cm³ for basalt (ρ_f is the fiber density).

The volume of the corroded part of fiber was estimated based on the condition

$$V_{f\tau\,c} = V_{f_0} - V_{f\tau\,in}, \qquad (5)$$

It can be seen in Fig. 3*a* that as d_f increases, the corroded fiber volumes decrease despite more intense absorption of CaO per fiber surface unit, and accordingly, the volume parts of intact fiber increase. This is presumably due to the fact that as the fiber diameter increases, the surface area of their contact with the aggressive medium perceptible decreases, other terms being equal.
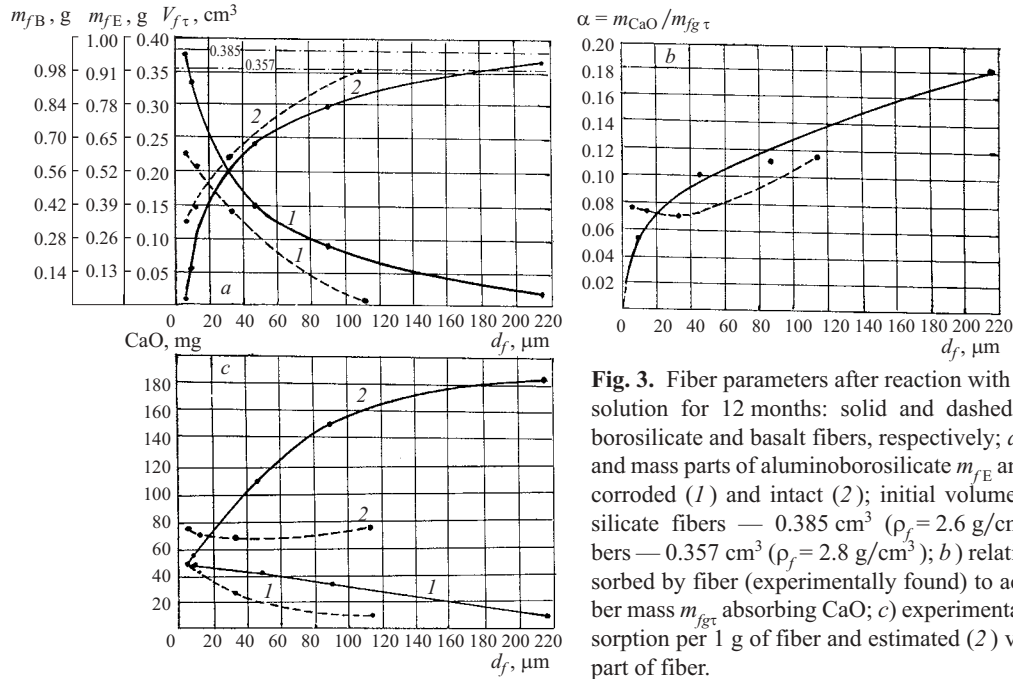
Fig. 3. Fiber parameters after reaction with saturated $Ca(OH)_2$ solution for 12 months: solid and dashed curves) alumino-borosilicate and basalt fibers, respectively; a) volume parts $V_{f\tau}$ and mass parts of aluminoborosilicate m_{fE} and basalt m_{fB} fibers corroded (1) and intact (2); initial volumes of aluminoboro-silicate fibers — 0.385 cm^3 ($\rho_f = 2.6$ g/cm^3) and basalt fibers — 0.357 cm^3 ($\rho_f = 2.8$ g/cm^3); b) relationship of m_{CaO} absorbed by fiber (experimentally found) to actual (corroded) fiber mass $m_{fg\tau}$ absorbing CaO; c) experimental data (1) CaO absorption per 1 g of fiber and estimated (2) values per corroded part of fiber.

It was suggested in [15] that the mass of CaO absorbed by fiber and the fiber mass $m_{fg\tau}$ absorbing the specified amount of m_{CaO} are related by the following dependence:

$$m_{CaO} = \alpha m_{fg\tau},$$

where α is the correlation coefficient.

Figure 3b shows variations in α for the considered fibrous after holding them in a saturated $Ca(OH)_2$ solution. The values m_{CaO} were taken from the data in [3] and $m_{fg\tau}$ were determined taking into account condition (5) from the expression

$$m_{fg\tau} = V_{f\tau c}\rho_f. \qquad (6)$$

It should be noted that experiments in measuring quantities of CaO absorbed per fiber mass unit performed by various researchers are somewhat arbitrary. It is clear that the actual amount of m_{CaO}, up to a certain limiting moment, is absorbed (formula (6)) only by a part of the fiber mass unit, which is actually subjected to corrosion. Therefore, the measured values of CaO mass absorbed by 1 g of fiber should be, strictly speaking, referred to the mass determined in expression (6). The real values of CaO mass referred to the specified (corroded) part of the fiber mass are significantly higher than the CaO mass referred to 1 g of fiber (Fig. 3c).

The reaction between alkaline metal hydroxides and glass silica is the crucial process in fiber corrosion, which has a substantial effect on the formation of the carrying skeleton of fiber materials. [2]. Considering this, we obtain

$$m_{CaO}/m_{SiO_2} = M_{CaO}/M_{SiO_2} = 56.08/60.1 = 1/1.07, \quad (7)$$

where M_{CaO} and M_{SiO_2} are the masses of CaO and SiO_2, g/mole.

Consequently, each CaO mass units reacts with 1.07 units of SiO_2 mass. Destruction of the silica skeleton leads to weakening (diminishes the strength) of the other structure-forming glass components bonded to that skeleton. In this process $1.07/\mu_{SiO_2}$ units of the glass mass is destroyed (μ_{SiO_2} is the relative content of SiO_2 in glass). For instance, μ_{SiO_2} in alkali-free aluminoborosilicate fibers in our experiments amounted to 0.54 and in basalt fiber it amounted to 0.51.

Taking this into account and using relationship (7), it is possible to determine the thickness of the conventional layer destroyed by corrosion in reaction with saturated $Ca(OH)_2$ solution:

$$V_{f\tau c} = \frac{1.07 m_{CaO}}{\rho_f \mu_{SiO_2}} = St,$$

hence

$$t = \frac{1.07 m_{CaO} \times 10^4}{\rho_f \mu_{SiO_2}}, \qquad (8)$$

where $V_{f\tau c}$ is the volume of the corroded fiber layer; m_{CaO} is the mass of absorbed CaO (mg/cm^2); S is the fiber surface, cm^2/g; ρ_f is the fiber density mg/cm^3; t is the thickness of the conventional corrosion layer, μm.

It is seen from formula (8) that t is proportional to an absorbed CaO mass.

The coefficient m_{dur}, taking into account the decrease in the strength of fiber elements in fiberglass-cement with time, is equal to
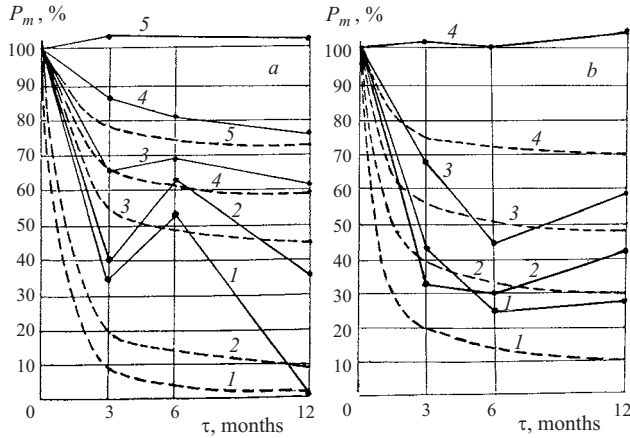
$$m_{dur} = N_\tau/N_0$$

Fig. 4. Time changes of experimental (solid curves) and estimated (dashed curves) strength values P_m of fibers under the effect of saturated $Ca(OH)_2$ solution: *a*) aluminoboron fibers of diameters 6.5 (*1*), 10.3 (*2*), 46.0 (*3*), 90.1 (*4*), and 291.0 (*5*) μm; *b*) basalt fibers of diameters 6.7 (*1*), 15.1 (*2*), 33.4 (*3*), and 117.0 μm (*4*).

or

$$m_{dur} = \frac{P_0 \pi r_{f\tau}^2}{P_0 \pi r_{f_0}^2} = \left(\frac{r_{f_0} - t}{r_{f_0}}\right)^2 = \left(1 - \frac{t}{r_{f_0}}\right)^2, \qquad (9)$$

where r_{f_0} is the initial fiber cross-section radius; $r_{f\tau}$ is the radius of working (effective) cross-section of fiber at the time moment τ.

Thus the problem is reduced to finding a relationship to determine the conventional layer thickness, which dissolves (is corroded) under the effect of the products of hydration of cement binder. It follows from the performed analysis that the thickness of the specified layer depends on two factors: duration of the effect of the alkali medium formed in curing of cement stone (simulated by the effect of saturated calcium hydroxide solution) and specific surface area of contact between the fiber and the alkali medium, i.e., the initial fiber diameter, all other terms being equal,

The function $t = f(\tau)$ has an ascending nature, however, growth intensity with time becomes significantly weaker.

Analysis of experimental data indicates that the effect of time on the considered processes can be reflected by the function

$$f(\tau) = \frac{4\tau}{3\tau + \bar{\tau}}, \qquad (10)$$

where τ is the current time, months; $\bar{\tau}$ is the time after which the intensity of growth of the conventional corrosion layer becomes perceptibly lower.

The time $\bar{\tau}$ is different for fibers of different chemical compositions. The values of the time function $\varphi(t)$ according to formula (10) vary from 0 to 1 at $\tau \le \bar{\tau}$ and from 1 to $4/3 = 1.33$ at $\tau \ge \bar{\tau}$ (at $\tau = \infty$ the function $\varphi(t)$ asymptotically approaches the value 1.33).

The function of the effect of the fiber diameter on the conventional layer thickness $t = f(d_f)$ can be represented in the following form:

$$f(d_f) = \sqrt{d_{f_0}}.$$

Thus, the thickness of the conventional fiber layer subjected to corrosion is equal to

$$t = K \frac{4\tau}{3\tau + \bar{\tau}} \sqrt{d_{f_0}}. \qquad (11)$$

In doing so, the coefficient K and $\bar{\tau}$ are selected for each material comprising the fiber (for the respective chemical composition of fiber) and their values are constant for the fiber materials.

Based on analysis of experimental data [3], the values K and $\bar{\tau}$ were obtained for the considered aluminoborosilicate and basalt fibers (Table 1). Table 1 also lists the values K and $\bar{\tau}$ for fibers Shch-15-ZhT, STs-6, ShchS-1 and Cem-Fil, which were determined based on experimental data of the TsNIIpromzdanii JSC and the Stekloplastic Research-and-Production Company.

Taking into account expressions (9) and (11), we obtain a formula for estimating the coefficient m_{dur} :

$$m_{dur} = \left(\frac{r_{f_0} - K \frac{4\tau}{3\tau + \bar{\tau}} \sqrt{d_{f_0}}}{r_{f_0}}\right)^2, \qquad (12)$$

where the values of K and $\bar{\tau}$ are taken from Table 1.

A correlation of experimental [3] and calculated dependences $\gamma = f(N_\tau / N_0) = m_{dur}$ expressed via P_m indicates (Fig. 4) that formula (12) with the values K and $\bar{\tau}$ taken from Table 1 satisfactorily generalizes experimental data.

Dependence (12) was also tested by correlating the calculation results with experimental data of other researchers [6 – 11, 3, 14, 17]. The correlation results for different types of fibers are listed in Table 2 and for fiberglass cement samples in Table 3. During this verification, in addition to testing fibers in saturated $Ca(OH)_2$ solution [1] and their subsequent rupture at preset time moments, other experiments were considered as well, in which fibers were exposed in portland ce-

TABLE 1

Fiber	K	$\bar{\tau}$, months	Deviation of value $\gamma = N_\tau / N_0$ ($\tau = 5$ years) for fiber of diameter, μm				
			10	25	50	100	200
Alumino-borosilicate	0.90	3	0.06	0.28	0.44	0.58	0.69
Basalt	0.70	3	0.18	0.40	0.55	0.66	0.76
Shch-15-ZhT	0.60	6	0.26	0.47	0.61	0.72	0.79
STs-6	0.50	6	0.36	0.55	0.67	0.76	0.83
ShchS-1	0.45	6	0.40	0.59	0.71	0.78	0.85
Cem-Fil	0.40	6	0.45	0.62	0.73	0.81	0.86

TABLE 2

Type of fiberglass	Fiber diameter, μm	Type of testing	Testing duration,* months	γ_{exp}	γ_{calc}	$\dfrac{\gamma_{exp}}{\gamma_{calc}}$	Published source
E	10.0	Effect of saturated solution Ca(OH)$_2$	12.0	0.120	0.090	1.33	[1]
	10.0	In a portland cement cassette at temperature 50°C	18.8	0.080	0.077	1.04	[6]
	10.0	The same at 70°C	133.0	0.040	0.060	0.67	[6]
	12.0	In air medium at 20°C	6.0	0.166	0.166	1.00	[10]
	14.0	In simulation solution at temperature 50°C	5.0	0.310	0.180	1.72	[11]
	14.0	In water at temperature 50°C	9.0	0.240	0.180	1.33	[11]
	10.0	The same	9.0	0.079	0.100	0.79	[12]
ShchS-1	8.0	Effect of saturated solution Ca(OH)$_2$	6.0	0.650	0.570	1.14	[1]
Shch-15-ZhT	60.0	The same	12.0	0.870	0.680	1.28	[1]
	10.0	In a portland cement cassette at temperature 50°C	18.8	0.400	0.290	1.38	[6]
	12.0	The same	16.0	0.350	0.348	1.01	[7]
	10.5	"	16.0	0.370	0.315	1.17	[7]
	11.6	"	31.0	0.240	0.310	0.77	[7]
	10.0	The same at 70°C	133.0	0.200	0.250	0.80	[6]
	16.0	In cement stone after exposure at 50°C	9.0	0.810	0.450	1.80	[8]
	16.0	The same	9.0	0.470	0.450	1.02	[8]
	10.0	In water or in steam-air mixture at 50°C	36.0	0.940	0.270	3.48	[9]
	12.0	Heat treatment at 40°C for 20 h, after that normal conditions	12.0	0.373	0.360	1.04	[10]
	12.0	The same at 60°C for 16 h, after that normal conditions	12.0	0.360	0.360	1.00	[10]
	12.0	The same at 80°C for 11 h, after that normal conditions	12.0	0.320	0.360	0.89	[10]
	12.0	In water at 20°C	12.0	0.340	0.360	0.94	[10]
	8.0	In air medium at 20°C	12.0	0.385	0.360	1.07	[10]
	10.0	In water at 50°C	9.0	0.470	0.350	1.34	[12]
Cem-Fil	10.0	In water or in steam-air mixture at 50°C	36.0	0.870	0.460	1.89	[9]
	15.0	In simulation solution at 50°C	5.0	0.680	0.640	1.08	[11]
	15.0	In water at 50°C	9.0	0.630	0.640	0.98	[11]
	10.0	The same	9.0	0.630	0.520	1.21	[12]

* Estimated time is converted to the testing time at 20°C.

ment cassettes in an equilibrium solution at an elevated temperature (50°C) [7], in cement stone after exposure in a steam chamber at temperature of 50°C [9], in a portland cement matrix with thermal treatment of samples in different conditions of temperature rise, exposure, and cooling, with temperature reaching 40, 60, and 80°C, or by exposure in water [10].

Relationship [10] was used to extrapolate data obtained at elevated temperatures to the service temperature of 20°C [2]:

$$\tau_1 = \tau_2 / K^{\frac{t_1 - t_2}{10}},$$

where τ_1 is the duration of heat-moisture treatment; τ_2 is the duration of treatment at 20°C; t_1 is the temperature of heat-moisture treatment; $t_2 = 20°C$; K is coefficient whose values vary for different fiber compositions from 2.62 to 2.69 (on the average K can be taken equal to 2.66).

Hence

$$\tau_2 = \tau_1 \times 2.66^{\frac{t_1 - t_2}{10}}.$$

In correlating experimental data and estimated values γ' (Table 3) for fiberglass-cement (fiberglass-concrete) sam-

ples, the tensile strength R^{τ}_{fbt} and the bending strength M^{τ}_{fb} of samples in time was determined:

$$R^{\tau}_{fbt} = m_1 \, \mu_f R_f k_{or} \, k_l \, m_{dur};$$

$$M^{\tau}_{fb} = R^{\tau}_{fbt} \, \omega (h - x) bz,$$

where $m_1 = f(\mu_f, R_b)$; μ_f is the volume content of fibers in the sample; R_b is the compressive strength of concrete:

$$R_b = R_{b28} \frac{\log \tau}{\log 28}; \qquad (13)$$

R_{b28} is the strength of concrete at the age of 28 days; R_f is the estimated tensile resistance of fiber; k_{or} is the fiber orientation coefficient; k_l is a coefficient taking into account the effect of the fiber length; m_{dur} is a coefficient taken from formula [10]; ω is the coefficient of completeness of the epure of the stretched zone of samples, $\omega = 0.5 + 2.5 R_{fbt}/R_{fb}$ (R_{fb} is the compression resistance of samples taking into account relationship (13); h and b are the height and width of the normal cross-section of the sample; x is the compressed zone

TABLE 3

Type of fiber in sample	Testing type	Exposure conditions before testing	Testing duration, months	$\gamma'_{\exp}$	γ'_{calc}	$\dfrac{\gamma'_{\exp}}{\gamma'_{\text{calc}}}$	Published source
ShchS-1	Bending	Normal air-moisture	12	0.69	0.52	1.33	[1]
Shch-15-ZhT	The same	The same	88	0.39	0.32	1.22	[5]
"	"	"	51	0.44	0.31	1.40	[5]
"	"	"	36	0.60	0.33	1.80	[14]
"	"	"	9	0.68	0.42	1.62	[14]
"	"	In water	9	0.51	0.42	1.21	[14]
"	"	The same	12	0.73	0.50	1.46	[17]
Cem-Fil	Tensile	In water	60	0.68	0.56	1.19	[4]
	Bending	The same	60	0.55	0.80	0.69	[4]
	The same	Normal air-moisture	51	0.64	0.55	1.16	[5]
	Tensile	The same	60	0.81	0.65	1.25	[13]

height; z is the inner force couple arm; at $\omega = 1$ $z = h/2$; at $\omega = 0.5$ $z = 2(h - x)/3 + 0.5x$.

Taking into account the above formulas, the tensile

$$\gamma'_{\text{calc}} = R^{\tau}_{f\,bt}/R^{0}_{f\,bt}$$

and bending relationships for the samples were determined:

$$\gamma'_{\text{calc}} = M^{\tau}_{f\,b}/M^{0}_{f\,b}$$

(indexes 0 and τ correlate with the initial and long-time strength of samples, respectively).

It is seen from data in Tables 2 and 3 that the proposed analytical relationship reflected in formula (12) correlates sufficiently well with the results obtained in the experiments (mostly within the limits of $\pm 30\%$).

Table 1 taking into account calculations based on formula (12) gives an example of predicted variations in fiber strength at the age of 5 years.

Calculation also shows that at the age of 10 years the expected values of sample strength compared to the data in Table 1 will change only in the second or third decimal place. The predicted strength variations agree well with experimental relationships (reflect the kinetics of the processes) and indicate that the strength of all the considered types of fibers decrease under the effect of an alkali medium of hydrated cement; however, this process in general is attenuating. It is also obvious that the larger the fiber diameter, the less perceptible is the decrease in strength and the difference between the strength loss values in fibers of different chemical compositions. This fact is rather significant, as it shows that fiberglass cement composites can be produced using different modifications of reinforcing fibers, considering the rational selection (depending on particular engineering and economic purposes) of their chemical compositions and diameters.

The proposed method for predicting the carrying capacity of composites based on cement matrixes with reinforcing components represented by different types of fibers can be used in designing fiberglass cements for construction intended for long-time service, taking into account expected variations in strength of fibers and of proper composites.

REFERENCES

1. F. N. Rabinovich and N. D. Klishanis, "Resistance of glass fibers to the effect of hydrated cement medium," *Izv. Akad. Nauk SSSR, Ser. Neorg. Mater.*, No. 2, 323 – 329 (1982).
2. A. A. Pashchenko, V. P. Serbin, A. P. Paslavskaya, et al., *Reinforcement of Inorganic Binding Materials by Mineral Fibers* [in Russian], Stroiizdat, Moscow (1988).
3. F. N. Rabinovich, V. N. Zueva, and L. V. Makeeva, "Resistance of basalt fibers in a hydrated cement medium," *Steklo Keram.*, No. 12, 29 – 32 (2001).
4. "A study of properties of CemFil – portland-cement composite," in: *Fiber-Reinforced Materials* [Russian translation], Stroiizdat, Moscow (1982), pp. 60 – 77.
5. D. L. Orlov and G. V. Leuta, "A study of strength parameters of composite materials after long-time storage," in: *Publ. of GIS Institute* [in Russian] (1989), pp. 28 – 34.
6. S. G. Danilova, "On corrosion of fiberglass in portland cement stone," in: *Publ. of GIS Institute* [in Russian] (1989), pp. 8 – 13.
7. S. G. Danilova and E. A. Melikhova, "A method for determining the chemical resistance of complex glass filaments intended for reinforcement of articles based on a hydraulic binder," in: *Publ. of GIS Institute* [in Russian] (1985), pp. 14 – 20.
8. D. L. Orlov, G. E. Murashova, and N. V. Bareeva, "Development of fiberglass with a decreased content of ZrO_2 resistant in cement stone," in: *Publ. of GIS Institute* [in Russian] (1985), pp. 25 – 28.
9. Yu. V. Meitin and E. A. Mishina, "The use of small cement blocks method in estimating durability of fiberglass cement," in: *Publ. of GIS Institute* [in Russian] (1989), pp. 48 – 50.
10. Sh. Ya. Izmailov, "The effect of technological factors on the efficiency of using fiber in fiberglass concrete," in: *Publ. of GIS Institute* [in Russian] (1989), pp. 44 – 47.
11. D. L. Orlov, G. E. Murashova, N. G. Chuvaeva, and N. V. Bareeva, "Production of cement-resistant fiberglass based on eudiolite lubricant," in: *Publ. of GIS Institute* [in Russian] (1989), pp. 3 – 6.

12. Yu. V. Meitin, "A method for determining the resistance of glass filaments in cement stone," in: *Publ. of GIS Institute* [in Russian] (1985), pp. 8 – 13.
13. A. J. Majumadar, J. West, and L. J. Larner, "Properties of glass fibers in a cement stone medium," in: *Fiber-Reinforced Materials* [Russian translation], Stroiizdat, Moscow (1982), pp. 48 – 59.
14. S. G. Danilova and G. V. Leuta, "Estimation of chemical resistance of fiberglass in portland cement matrix," *Publ. of GIS Institute* [in Russian] (1985), pp. 30 – 37.
15. F. N. Rabinovich, "A method for determining the resistance of glass fibers to the effect of hydrated cement medium," in: *Building Structures and Materials, Issue 2* [in Russian], VNIINTPI (1992), pp. 37 – 43.
16. F. N. Rabinovich, "A study of durability of fiberglass cement," in: *Theory of Structural Design. Building Structures and Materials, Issues 3 – 4* [in Russian], VNIINTPI (1992), pp. 27 – 33.
17. G. V. Leuta, "A study and development of chemically resistant glass using celestine concentrate," *Publ. of GIS Institute* [in Russian] (1989), pp. 16 – 20.